# Supporting Information
# for
# Anomalous surface diffusion of protons on lipid membranes

Running Title: Anomalous proton surface diffusion

Maarten G. Wolf, Helmut Grubmüller and Gerrit Groenhof

## Gs(r,t)

In addition to the time-dependence of the msd, also the self-part of the van Hove correlation function $G_s(\mathbf{r}, t)$ is an interesting measure to characterize anomalous diffusion. Here, $G_s(\mathbf{r}, t)$ is the probability that a particle has moved within a time span $t$ a distance $r$. The $G_s(\mathbf{r}, t)$ for a proton on a surface (figure S1) shows that the surface displacement exhibits long-tailed behavior with respect to a normal distribution, indicating anomalous surface diffusion.

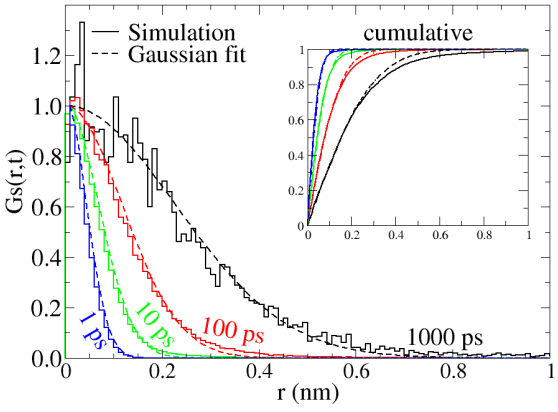


Figure S1: Gs(r,t) of a proton on a membrane surface. The gaussian fits correspond to a normal distributed surface displacement, and the simulation data represent the observed surface displacement.

## Periodic image contribution to autocorrelation function

The autocorrelation function of the hydronium-lipid hydrogen bonds gives the probability that after a certain time interval $t$ the hydronium forms a hydrogen bond with the same lipid. Because we used periodic boundary conditions in our simulation, it is possible that

the proton binds to the periodic image of this lipid. As a result, the autocorrelation function would reach a constant value between zero and one, rather than decay to zero.

In our simulations, the probability that the hydronium-lipid hydrogen bond was reformed with a periodic image was negligible. We obtained this probability from the two dimensional diffusion equation, which yields a distribution of 2D displacement,

$$d_{\text{molecule}}(r,t) \sim r \exp(-r^2/4Dt), \tag{1}$$

with $4Dt$ the 2D msd at time $t$ and $r$ the displacement. After normalization of the lipid phosphor and the hydronium distribution, the probability to encounter a periodic image after time $t$ was

$$p(t) = \int_0^{r_{\text{box}}} d_{\text{H}_3\text{O}^+}(r,t) \cdot d_{P_{\text{lipid}}}(r_{\text{box}} - r, t) dr \tag{2}$$

with $r_{\text{box}}$ the smallest box vector (finite size). For instance, at $t = 300$ ps, equation 2 yielded a probability of $10^{-13}$ for a hydronium in the hb1 ensemble to interact with a periodic image lipid. In the hb2 and hb3 ensemble this probability was even smaller, due to the smaller msd of the hydronium.

## Simplified model

In our atomisic simulation of an excess proton in the vicinity of a lipid membrane we find a non-linear relation between the proton mean square surface displacement and time, characterized by an initial subdiffusive regime that was followed by a small superdiffusive regime (Figure 4). The diffusion of a proton over a lipid membrane was thus highly anomalous, in contrast to the standard Fickian diffusion observed for a proton moving through bulk solvent.

Multiple phenomena are contributing to the highly anomalous surface diffusion of the proton. First, protons that are bound to a lipid followed the lipid's self-diffusion pattern within the bilayer, which is subdiffusive at short timescales (upto 50 ns) [1]. Second, protons that are trapped in a free-energy well on the surface experienced a local caging effect, which, in combination with a low percolation rate, also leads to a subdiffusive regime [2, 1]. Finally, the strong surface affinity of the proton, with the occasional bulk-mediated long diffusion pathway, typically leads to a superdiffusive regime [3]. The key aspect in these three phenomena is a favorable interaction between the lipids and the proton that results in a reduction of freedom of surface movement. The latter leads to the highly anomalous surface diffusion of the proton.

Remarkably, figure 4 shows that the superdiffusive regime was present only shortly within our simulations and the diffusion quickly became normal (*i.e.* Fickian), rather than extending over a long time-period and approaching the bulk diffusion coefficient [3]. To address this issue, we turned to a simplified model and focused on solutions of the

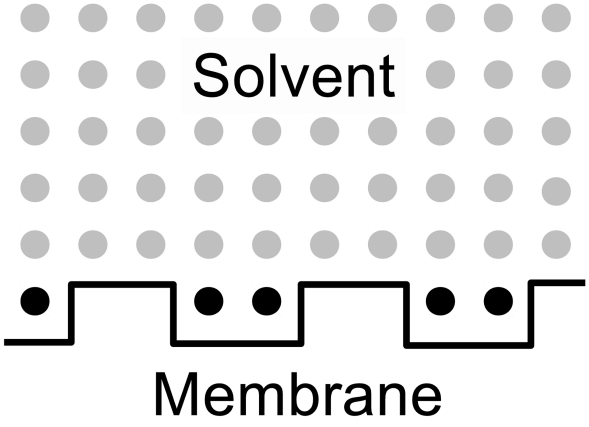


Figure S2: Illustration of the grid used to solve the diffusion equation. Accessible gridpoints are represented by spheres. Black spheres have a lower free-energy than gray spheres. Here, a small part of the grid with a well size of 2 gridpoints is shown.

diffusion equation (equation 3), modeled according to the characteristics of our atomistic simulations. Since the free-energy of the proton is not equal throughout the whole system (*i.e.* there is a surface affinity), the flux $J$ in the diffusion equation depends on the chemical potential gradient.

$$\frac{\delta c(r)}{\delta t} = \nabla J \tag{3}$$

$$= \nabla M c(r) \nabla \mu(r) \tag{4}$$

where $\mu(r)$ and $c(r)$ are the chemical potential and the concentration of the excess proton at location $r$, respectively, $M$ is a coefficient equivalent to the diffusion coefficient in Fick's diffusion equations, and $\nabla$ represents the vector differential operator del.

We solved the diffusion equation for a 2 dimensional system numerically. Therefore, the evolution of an initial point density on the surface was approximated by performing small timesteps on a grid (figure S2), where we utilized boundary conditions based on the results of our atomistic simulations. The presence of the membrane was represented by an excluded volume for $y < 0$, and the protons surface affinity by a lower free energy associated to the grid points directly adjacent to the excluded volume. To reduce the computational overhead, we used a bulk-to-surface free energy difference of -8 kJ mol$^{-1}$ instead of -13 kJ mol$^{-1}$, thereby shortening the manifestation of the anomalous diffusion regime. To create the energy wells on the surface that trap the protons, the excluded volume was protruded into the surface adsorption layer periodically. For simplicity, we omitted the proton binding to a lipid molecule and, consequentially, we expected a subdiffusive regime corresponding to the caging effect and a superdiffusion regime due to the occasional bulk-mediated diffusion pathway.

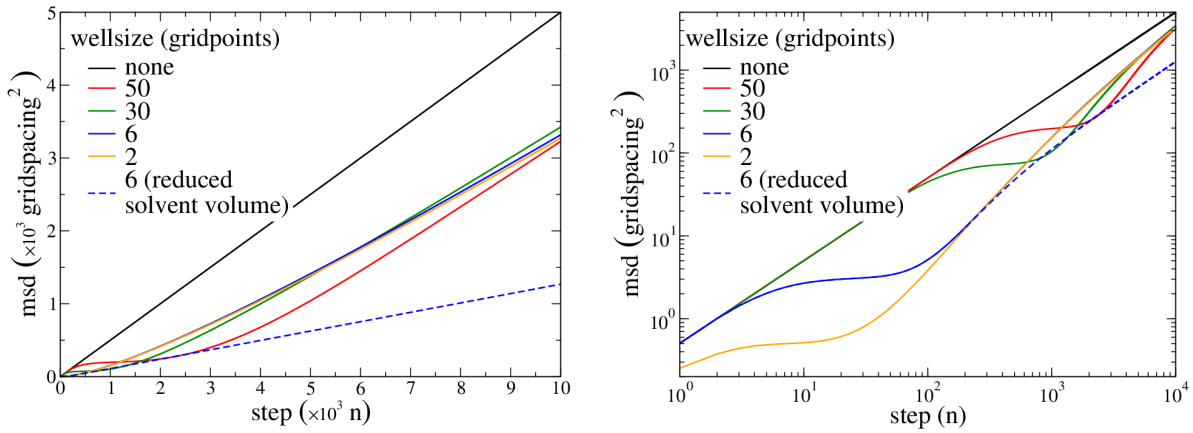


Figure S3: Numerical solutions to the differential equation describing proton diffusion in the vicinity of an adsorbing membrane. The gridsize was `600x600`, the free energy difference between surface and solvent was -8 kJ $mol^{-1}$, $M$ in the bulk was set to 1 $gridpoint^2$ $step^{-1}$ and the well-size was varied.

The mean square surface displacement of a proton in this simplified system displayed the same characteristic subdiffusive and superdiffusive regimes that we observed in the atomistic simulations (figure S3). Especially the system with a wellsize of 6 gridpoints compared very well to the results of the atomistic simulations.

In a further comparison between the solution of the diffusion equation and the atomistic simulations we found a discrepancy in the time-dependent diffusion coefficient (figure S4). The diffusion coefficient in the atomistic simulations quickly levels off in the course of our simulations, whereas the diffusion coefficient in the simplified model keaps on increasing and asymptotically approaches the linear diffusion coefficient of the no-well system. A major difference between the coarse-grained model and the atomistic simulations is the use of periodic boundary conditions in the latter. As a result, a periodic image membrane is present at short distance. After adding a second membrane in the coarse-grained model, the time-dependent diffusion coefficient (dashed line in figure S4) compares much better to that obtained from atomistic simulations. Thus, the periodic image membrane limits the length of the proton bulk excursions, which reduces the contribution of the bulk-mediated diffusion, shortening the superdiffusive regime.

## How to experimentally validate bulk-mediated surface diffusion

In this section we propose a possible experiment to distinguish between bulk-mediated and on-surface diffusion of a proton over a membrane. Since the fundamental difference between these two diffusion modes is whether or not a superdiffusive regime appears, we

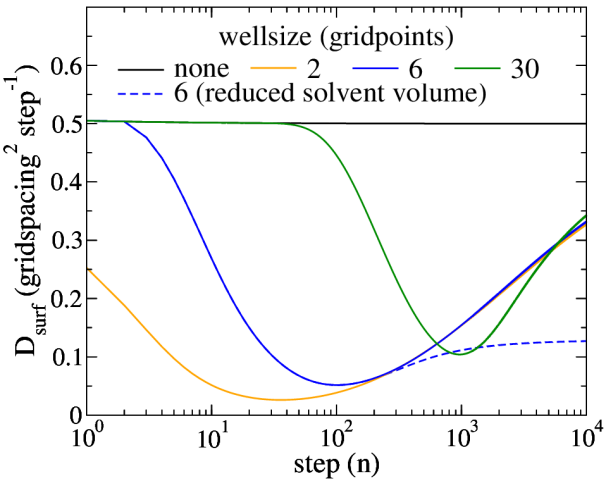


Figure S4: Time dependent diffusion coefficient for surface diffusion on a model membrane. For model parameters see figure S3.

focussed on this aspect in the design of the experiment.

A clear difference between superdiffusion and normal diffusion is the relation between time and msd. On the one hand, a superdiffusion regime leads to a super-linear relation, whereas, on the other hand, normal (Fickian) diffusion leads to a linear relation. By measuring the travel time between a proton source and a proton sensor for various distances, it is possible to experimentally measure the msd as a function of time, and thus to determine the predominant diffusion mode within the measured time- and lengthscale.

Before proposing an experiment we stress that the time- and lengthscale should match that of the onset of the expected superdiffusive regime, because the superdiffusive regime, which approaches a linear asymptot, is indistiguishable from standard diffusion at time- and lengthscale where the msd is close to this asymptot. In our simulations, the superdiffusive regime starts around 1 ns and stretches over an unknown period of time, with a corresponding lengthscale starting around 1 $nm^2$. Consequently, the experimental time and length scale that we are looking for are a few tens of ns and $nm^2$. On a lipid bilayer this is almost on the scale of a single lipid, which has a surface area of approximately 0.6 $nm^2$. Thus the distance between a proton source and a proton sensor can only be a few tens of lipids.

To control the distance between the proton source and the proton sensor on the nm length scale one can think of a rigid linker. Clearly, the resulting linked source and sensor cannot be allowed to interact with other linked pairs, which requires very low concentrations and careful design of the linker to avoid aggregation. This is a considerable challenge, but, if possible, a proper linker would allow the existence of a superdiffusive regime to be tested by varying the length of the linker within the relevant length scale. If the linker distance falls within the superdiffusive regime, a super-linear relation between the square

of the linker distance and the time of maximum sensor activity should be observed.

Alternatively, it may be easier to measure the mean distance traveled by the protons from source to sensor in order to determine the dominant diffusion mode. After a single proton is released on a lipid membrane the average length of the path traveled to reach a sensor will depend on the sensor concentration. Variation of the sensor concentration will change the average distance traveled to a sensor and can thus be used to experimentally determine the relation between time and mean squared displacement. Release and measurement of a single proton is impracticle, but, if one could control the distribution of proton sources into a regular evenspaced array, variation of the sensor concentration should similarly allow to distinguish between a superdiffusive and a normaldiffusive regime.

To determine how the difference in sensor signal will be manifested we modeled such an experimental setup by solving an extended diffusion equation,

$$\begin{aligned}
\frac{\delta c_{H^+}(r)}{\delta t} &= \nabla M c_{H^+}(r) \nabla \mu_{H^+}(r) && (5)\\
&\quad - k_{ass} c_{H^+}(r) c_{sensor}(r) + k_{diss} c_{sensorH}(r) && (6)\\
\frac{\delta c_{sensor}(r)}{\delta t} &= D \left( \frac{\delta^2 c_{sensor}(r)}{\delta x^2} + \frac{\delta^2 c_{sensor}(r)}{\delta y^2} \right) && (7)\\
&\quad - k_{ass} \mu_{H^+}(r) c_{sensor}(r) + k_{diss} c_{sensorH}(r) && (8)\\
\frac{\delta c_{sensorH}(r)}{\delta t} &= D \left( \frac{\delta^2 c_{sensorH}(r)}{\delta x^2} + \frac{\delta^2 c_{sensorH}(r)}{\delta y^2} \right) && (9)\\
&\quad + k_{ass} \mu_{H^+}(r) c_{sensor}(r) - k_{diss} c_{sensorH}(r) && (10)
\end{aligned}$$

assuming the following reaction between the proton and the sensor

$$\mathrm{H_3O^+} + \mathrm{sensor} \rightleftharpoons \mathrm{H_2O} + \mathrm{sensorH^+} \tag{11}$$

with $D$ the surface diffusion coefficient of the (protonated) sensor, which is treated as a constant. Note that the sensor is assumed to be part of the membrane and, hence, diffusion normal to the membrane is not taken into account.

We solved this set of diffusion equations in a similar manner as we did in the case of proton diffusion. We added the (protonated) sensor to the surface layer of our grid model, both inside and outside the wells. The proton association/ dissociation from a sensor located inside or outside a well was related to the surface layer or the bulk, respectively. Within the computational and model limits, we tried to resemble a real system as close as possible, but we note that both the large timestep and the significant simplification make a direct translation of our solution onto a target experiment unfeasible. Instead, our results should rather be interpreted qualitatively.

The diffusion equations were solved on a 80x80 grid using reflective boundary conditions. The gridspacing was 0.1 nm and the timestep 1 ns. The proton and sensor

displacement were set to $10^{-2}$ nm$^2$ ns$^{-1}$ and $10^{-5}$ nm$^2$ ns$^{-1}$, respectively. Proton adsorption to the surface was set equal to the proton bulk-displacement in one dimension, and proton desorption was derived from $e^{-\Delta G/kT} = \frac{k_{ads}}{k_{des}}$ with $\Delta G = -11.5$ kJ mol$^{-1}$. The proton-sensor association constant was set to 1 and the dissociation constant was calculated from $k_{diss} = k_{ass} \cdot K_A$ with $K_A$ the sensor acidity constant set to 6 for the bulk. A bulk pH of 8 was used, and the sensor surface concentration was varied between $10^{-5}$ and $10^{-1}$ molecules lipid$^{-1}$, where one lipid was assumed to occupy eight gridpoints.

The initial steady-state was disrupted by the release of one proton at the origin, corresponding to an approximate release concentration of 1 proton per 100 lipids. The enhanced proton concentration on the surface slowly decays, due to an increased association with the sensor as well as an increased surface desorption. Simultaneously, the concentration of the protonated sensor increases and the concentration of the unprotonated sensor decreases, until a new equilibrium is established. Since the surface desorption is a ceaseless process, this equilibrium cannot be maintained, and the concentration of the proton as well as the protonated sensor starts to fall, whereas the concentration of the unprotonated sensor begins to rise. This turning point in the (protonated) sensor concentration yielded a maximum in the sensors activity.

From the time dependence of the maximum sensor activity as a function of sensor concentration one can distinguish between normal- and super-diffusion. Indeed, when comparing the super-diffusion systems, *i.e.* the well systems, to a normal diffusion system, we observe a different decay profile of the $t_{max\_activity}$ upon increasing concentration (figure 12). Thus systems with a clear superdiffusive regime can be distinguished by the different decay in $t_{max\_activity}$, which is characterized by a second minimum or a shoulder in the plot of the powerlaw exponent $\alpha$ ($\delta \ln t_{max\_activity}/\delta \ln c_{sensor}$).

Regular 2D arrays of small colloidal particles on a substrate [4] may present a suitable base for the array of proton sources; a hydrophobic caged proton (6,7-dimethoxycoumarin-4-yl) [5, 6] can be used as an instantaneous proton source; and Fluorescein [5, 6, 7, 8] or OregonGreen [8] linked to a lipid can be used as a proton sensor.

We remark that an experiment in which neither the proton source nor the proton sensor location is fixed cannot be used to distinguish between superdiffusion and normaldiffusion, because on average there is neither a source nor a sensor gradient on the surface, and, as a result, no net flux of either on the surface. This does not mean that the time to maximum activity cannot be different for distinct diffusion modes, rather the time to maximum sensor activity will not depend on the distance traveled between source and sink, and can thus not be used to find anomalous diffusion.

Finally, we also considered FCS to track the protons surface diffusion. FCS has the advantage that the proton diffusion can be measured in equilibrium [7], but since the diffusion model is used as input to interpret the autocorrelation function of the signal intensity, FCS is only useful if the diffusion mode is known.

## Hydroxide parameters

Figure S5 shows a figure of our hydroxide model with the values of the parameters.

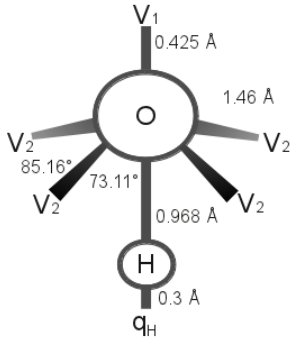


| | |
|---|---|
| $q_O$ (e) | -1.32 |
| $q_H$ (e) | 0.32[1] |
| $\epsilon$ (kcal/mol) | 0.0514 |
| $\sigma_O$ (Å) | - |
| $\sigma_{V1}$ (Å) | 2.916 |
| $\sigma_{V2}$ (Å) | 2.5 |
| $\sigma_{HH}$ (Å) | 1.1[2] / 1.4[3] |

[1]Positioned on $q_H$ site
[2]For combination rule 1
[3]For combination rule 2

Figure S5: Structure and non-bonded parameters of our hydroxide model.

## Radial distribution function of excess proton in water

To verify whether HYDYN describes the properties of the excess proton in water, we performed HYDYN simulations of the hydrated proton in a small water box and analyzed the trajectory. The intermediate transfer congurations such as the pseudo-Zundel complex, which are observed in a HYDYN simulation, are a clear distinction to non-reactive force field simulations. The consequences for the solvation structure are apparent from the radial distribution functions, shown in Figure S6.

Although the RDF contains the main features of experimental and *ab initio* MD RDFs, there are some differences. The first peak is too narrow and, since HYDYN captures the right coordination number of 3, also too high. The RDF contains a shoulder around 3.2 Å, associated with the waters in the lone-pair region, albeit less pronounced than in *ab initio* MD or MS-EVB3 [9, 10]. The peak for the second solvation shell is present, but at too high value. Including polarization (via the SWM4-NDP model) improves the situation somewhat and brings this peak to slightly lower values. The diffusion constant of the excess proton in water at 300 K is $4.4 \cdot 10^{-5}$ $cm^2s^{-1}$,in line with MS-EVB3 results $2.8 \cdot 10^{-5}$ $cm^2s^{-1}$ and experiment $9.3 \cdot 10^{-5}$ $cm^2s^{-1}$. Therefore, while our model is less accurate than MS-EVB or CPMD with respect to the water structure, it is sufficiently accurate to capture the anomalous diffusion.

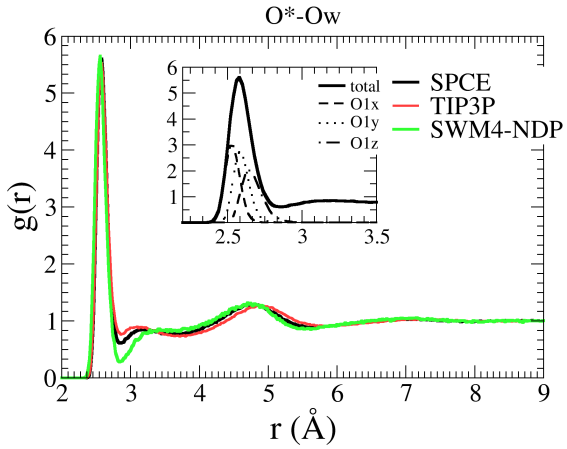


Figure S6: Radial distribution function for the donor-acceptor Oxygen atoms (O*-O) in a HYDYN simulation with different force fields.

# References


[1] E. Flenner, J. Das, M.C. Rheinstädter, and I. Kosztin. Subdiffusion and lateral diffusion coefficient of lipid atoms and molecules in phospholipid bilayers. *Phys. Rev. E*, 79:011907, 2009.

[2] Michael J. Saxton. Anomalous diffusion due to obstacles: A monte carlo study. *Biophys J*, 66:394–401, 1994.

[3] Oleg V. Bychuk and Ben O'Shaughnessy. Anomalous diffusion at liquid surfaces. *Phys Rev Lett*, 74:1795, 1995.

[4] Simon Ullrich, Sebastian P. Scheeler, Claudia Pacholski, Joachim P. Spatz, and Stefan Kudera. Formation of large 2d arrays of shape-controlled colloidal nanoparticles at variable interparticle distances. *Part. Part. Syst. Charact.*, 30:102–108, 2013.

[5] S. Serowy, S.M. Saparov, Y.N. Antonenko, W. Kozlovsky, V. Hagen, and P. Pohl. Structural proton diffusion along lipid bilayers. *Biophys. J.*, 84:1031–1037, 2003.

[6] A. Springer, V. Hagen, D.A. Cherepanov, Y.N. Antonenko, and P. Pohl. Protons migrate along interfacial water without significant contributions from jumps between ionizable groups on the membrane surface. *Proc. Natl. Acad. Sci. USA*, 108:14461–14466, 2011.

[7] M. Brändén, T. Sandén, P. Brzezinski, and J. Widengren. Localized proton microcircuits at the biological membrane-water interface. *Proc. Natl. Acad. Sci. USA*, 103:19766–19770, 2006.

[8] T. Sandén, L. Salomonsson, P. Brzezinski, and J. Widengren. Surface-coupled proton exchange of a membrane-bound proton acceptor. *Proc. Natl. Acad. Sci. USA*, 107:4129–4134, 2010.

[9] C. Knight, C.M. Maupin, S. Izvekov, and G.A. Voth. Defining condensed phase reactive force fiels from ab initio dynamics simulations: the case of the hydrated excess proton. *J. Chem. Theory Comput.*, 6:3223–3232, 2010.

[10] Yujie Wu, Hanning Chen, Feng Wang, Francesco Paesani, and Gregory A. Voth. An improved multistate empirical valence bond model for aqueous proton solvation and transport (vol 112B, pg 467, 2008). *J. Phys. Chem. B*, 112(23):7146, 2008.